

DOI: 10.1002/sml.200600098

## SiC-Shell Nanostructures Fabricated by Replicating ZnO Nano-objects: A Technique for Producing Hollow Nanostructures of Desired Shape\*\*

Jun Zhou, Jin Liu, Rusen Yang, Changshi Lao, Puxian Gao, Rao Tummala, Ning Sheng Xu, and Zhong Lin Wang\*

Hollow nanostructures have important applications due to their large outer and inner surfaces, as well as cavity-confined nanoscale reactions and transport processes. The simplest hollow structures are nanoparticle and nanotubes shells. Compared to solid nanoparticles or nanorods and nanowires, tubular nanostructures of inorganic materials have potential applications in biotechnology, such as drug delivery,<sup>[1]</sup> gene delivery,<sup>[2]</sup> gene therapy,<sup>[3]</sup> biosensors,<sup>[4,5]</sup> and bioanalysis and catalysis.<sup>[6]</sup> In addition, when the tubular structures are filled with special biomolecules, the structures may act as delivery channels for such molecules. The tubular structures are made either by direct growth<sup>[7]</sup> or by nanowire-templated epitaxial growth using metal-organic chemical vapour deposition (MOCVD).<sup>[8]</sup> Here, we extend the template-assisted method for fabricating shelled structures of nano-objects of desired shapes and configurations. Our technique is based on replicating ZnO-based nanostructures by SiC at low temperatures. Subsequent dissolution of ZnO leaves a SiC shell that preserves the same shape as the

original ZnO nanostructure. The SiC hollow nanostructures could be used as nanoreactors, molecular transporters, and more. The methodology demonstrated here can be extended to other types of shelled structures of different chemical compositions.

Silicon carbide is an important semiconductor in the fabrication of electronic devices operated at high temperature, power, and frequency and in harsh environments.<sup>[9]</sup> Several groups have reported the fabrication of one-dimensional (1D) SiC nanotubes using template-assisted growth methods at high temperatures.<sup>[10–12]</sup> Borowiak-Palen et al. produced SiC nanotubes based on high-temperature (1350 °C) reactions between silicon powders and multi-walled carbon nanotubes.<sup>[10a]</sup> Hu et al. formed SiC nanotubes by reacting CH<sub>4</sub> with SiO at ≈800 °C.<sup>[11]</sup> Sun et al. prepared SiC nanotubes by reacting SiO with carbon nanotubes at 1250 °C.<sup>[12]</sup> However, the high growth temperature limits the integration of the current growth method with semiconductor fabrication technology, which usually requires growth temperatures below 500 °C.

In recent years, our group has done much research on the growth of various ZnO nanostructures using a vapor-solid growth process.<sup>[13–20]</sup> Figure 1 shows the morphologies of selected ZnO nanostructures that were used as templates in the following experiments for fabricating SiC hollow structures. The nanobelts shown in Figure 1a have a uniform shape along their growth axis. Figure 1b shows the morphology of tin-catalyzed ZnO nanowires. The ZnO nanowires typically have a large tin catalyst at their tips (as shown in the left-hand inset of Figure 1b). The tin catalyst is much larger than the nanowire. In some cases, two ZnO nanowires share a single catalyst particle (right-hand inset of Figure 1b). Figure 1c–e shows the scanning electron microscopy (SEM) images of various ZnO nanostructures (combs, junctions, and helices, respectively).

The synthesis strategy of the SiC hollow nanostructures involved two steps, as shown in Figure 2. Firstly a SiC layer was deposited on the surface of the ZnO nanostructure templates to form ZnO–SiC core–shell nanostructures via plasma-enhanced chemical vapor deposition (PECVD). The source materials for SiC were CH<sub>4</sub> and SH<sub>4</sub> gases, and the deposition temperature was ≈250–300 °C. Secondly, the ZnO–SiC core–shell nanostructures were added to a dilute HCl solution (≈0.2 mol L<sup>-1</sup>) to remove the ZnO cores. Finally, only SiC tubelike nanostructures were left, retaining the corresponding shapes of the ZnO nanostructure templates.

Transmission electron microscopy (TEM) was used to reveal the shell structure of the replicated nanostructures. Figure 3a shows a typical TEM image of the ZnO–SiC core–shell nanobelt synthesized in this work. The ZnO nanobelt coated with a uniform SiC shell is clearly indicated based on the contrast of the TEM image. The shell along the ZnO nanobelt is uniform and smooth. In our experiments, the thickness of the layer can be tuned by adjusting the parameters in the PECVD process. Energy dispersive X-ray (EDX) analysis (inset of Figure 3a) revealed that the core–shell nanobelt is composed of Zn, O, Si, and C. No other elements were found, indicating that the shell on the

[\*] J. Zhou, J. Liu, R. S. Yang, C. S. Lao, Dr. P. X. Gao, Prof. Z. L. Wang  
School of Materials Science and Engineering  
Georgia Institute of Technology  
Atlanta, GA 30332-0245 (USA)  
Fax: (+1) 404-894-9140  
E-mail: zhong.wang@mse.gatech.edu

J. Zhou, N. S. Xu  
State Key Lab of Optoelectronic Materials and Technologies and  
Guangdong Province Key Laboratory of Display Materials and  
Technologies  
Sun Yat-Sen (Zhongshan) University, Guangzhou, 510275 (China)  
J. Liu, Prof. R. Tummala  
School of Electrical and Computer Engineering  
Georgia Institute of Technology  
Atlanta, GA 30332-0245 (USA)

[\*\*] Z.L.W. acknowledges the support of NSF grant DMR-9733160, the NASA Vehicle Systems Program, the Department of Defense Research and Engineering (DDR&E), and the Defense Advanced Research Projects Agency (Award No. N66001-04-1-8903). N.S.X. acknowledges the support of the National Natural Science Foundation of China, the Ministry of Science and Technology of China, the Education Ministry of China, the Department of Education and the Department of Science and Technology of Guangdong Province, and the Department of Science and Technology of Guangzhou City. J.Z. acknowledges the Kaisi Fund from Sun Yat-Sen University.

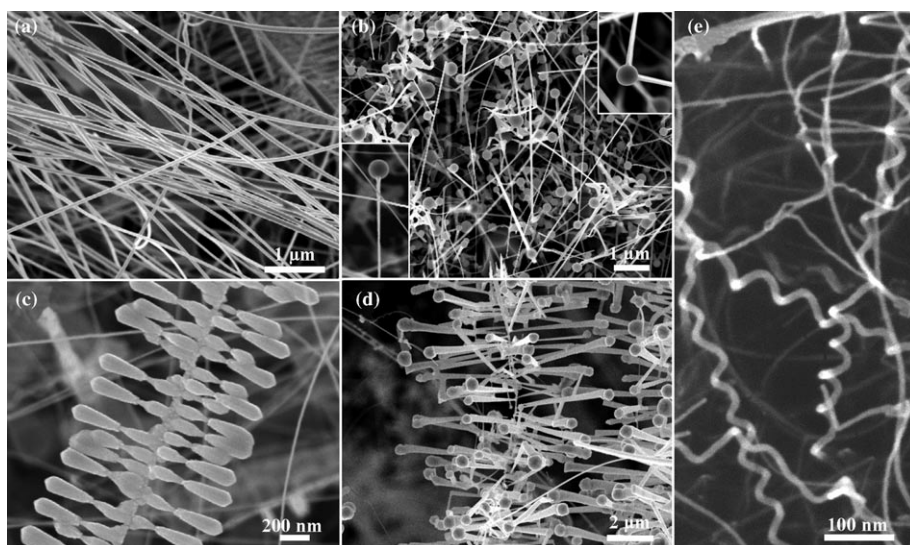


**Figure 1.** Scanning electron microscopy (SEM) images of various nanostructures used as templates in this work: a) ZnO nanobelts; b) tin-catalyzed ZnO nanowires; c) ZnO nanocombs; d) ZnO nanojunctions; e) ZnO nanohelices. Left-hand inset in (b) is a typical SEM image of tin-catalyzed ZnO nanowires with a large tin catalyst at the tip. Right-hand inset in (b) is an SEM image showing two ZnO nanowires sharing the same tin catalyst particle.

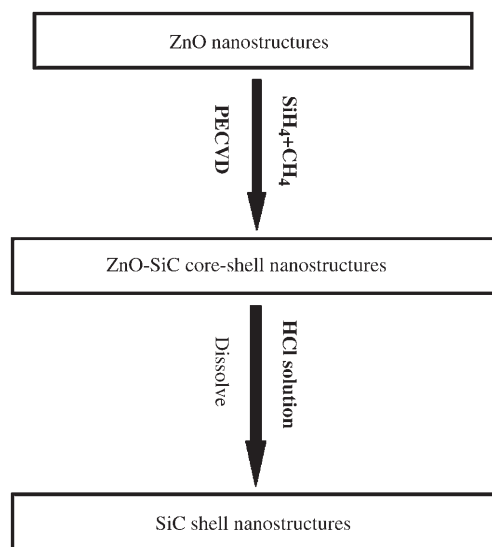


**Figure 2.** Schematic diagram showing the fabrication process of SiC-shell nanostructures using ZnO nano-objects as templates.

outer surface of the ZnO nanobelt is SiC. Figure 3b and c shows two high-quality SiC nanotubes made by the technique. The inner dimension of the SiC nanotube is determined entirely by the size of the ZnO nanobelt. Figure 3d shows a TEM image of many SiC nanotubes, indicating that SiC nanotubes can be fabricated simultaneously for a large group of nanobelts. The selective area electron diffraction (SAED) pattern (inset of Figure 3d) taken from the as-made SiC nanotubes shows that the as-synthesized SiC nanotubes are amorphous due to the low growth temperature. Moreover, the absence of diffraction spots due to the crystalline ZnO nanobelt templates proves that the ZnO cores were completely removed, and that the remainder were entirely SiC nanotubes.

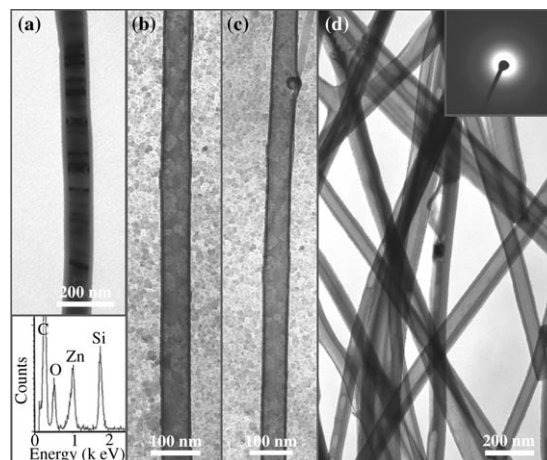


**Figure 3.** a) Transmission electron microscopy (TEM) image of the ZnO-SiC core-shell nanobelt. The lower image shows an energy dispersive X-ray spectrum (EDX) from the ZnO-SiC core-shell nanobelt, indicating the presence of Zn, O, Si, and C in the structure. b, c) TEM images of two high-quality SiC nanotubes; d) TEM image of many SiC nanotubes after removal of the ZnO core. The inset is a selective area electron diffraction (SAED) pattern of the ZnO nanotubes.

other SiC nanotube. The image contrast indicates that the SiC nanotube is hollow. In addition, V-shaped SiC nanotubes were also formed in this work, as shown in Figure 4d and e. Comparing their shape to the morphology of the structure of two nanowires sharing a single catalyst particle, as shown in the top-right corner of Figure 1b, it is apparent that the original shape is fully replicated by SiC.

Our technique can also produce shell structures of complex nano-objects. Figure 5 shows TEM images of SiC-shell nanocombs formed using ZnO nanocombs as templates. The inset in Figure 5d is a dark-field TEM image of a SiC nanocomb shell, the contrast of the image indicating the hollow

Figure 4a shows a typical TEM image of a tin-catalyzed ZnO-SiC core-shell nanowire. When the ZnO cores and the tin catalysts were removed by HCl solution, high-quality SiC nanotubes were produced (Figure 4b). Notably, the SiC nanotube has a large, hollow ball at the tip, which is due to the Sn ball at the tip of the ZnO nanowire. This type of structure may be useful as a ‘nanothermometer’, which was first demonstrated by filling carbon nanotubes with Ga.<sup>[21]</sup> Figure 4c and d shows bright-field and dark-field TEM images, respectively, of an

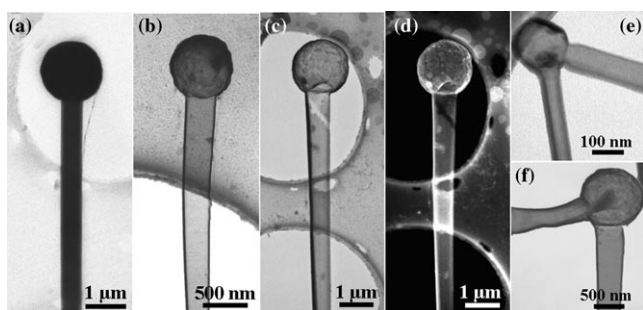


**Figure 4.** a) TEM image of a tin-catalyzed ZnO-SiC core-shell nanowire; b) TEM image of a high-quality SiC nanotube with an enclosed large hollow ball at the tip; c, d) bright-field and dark-field TEM images of a SiC nanotube, respectively; e, f) TEM images of two V-shaped SiC nanotubes.

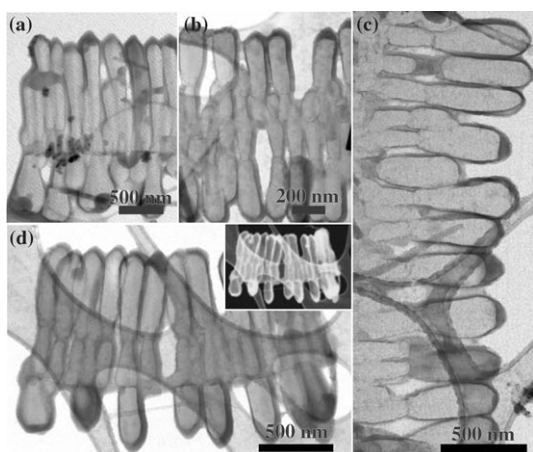


**Figure 5.** TEM images of SiC-shell nanocombs. Inset in (d) is a dark-field TEM image of a SiC hollow nanocomb.

structure of the nanocomb. Furthermore, based on the TEM observations, we find that both the teeth and body of the SiC-shell nanocomb appear to be closed. Figure 6a and b shows two L-shaped SiC junctions. Figure 6c and d shows two shell-structured multijunctions fabricated using ZnO nanojunctions as templates. The arrowheads in Figure 6d in-

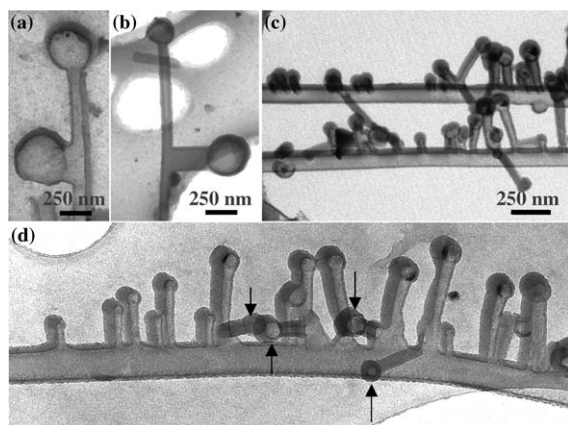


**Figure 6.** TEM images of SiC-shell nanojunctions: a, b) SiC hollow nanojunctions with a single junction; c, d) SiC-shell three-dimensional nanojunctions with multijunctions.

dicating the three-dimensional character of the SiC-shell nanojunctions.

We have also produced some novel SiC-shell nanostructures, such as hollow nanohelices. We have previously reported nanohelices consisting of 10-nm ZnO nanowires.<sup>[18]</sup> Figure 7a shows typical TEM images of the as-synthesized

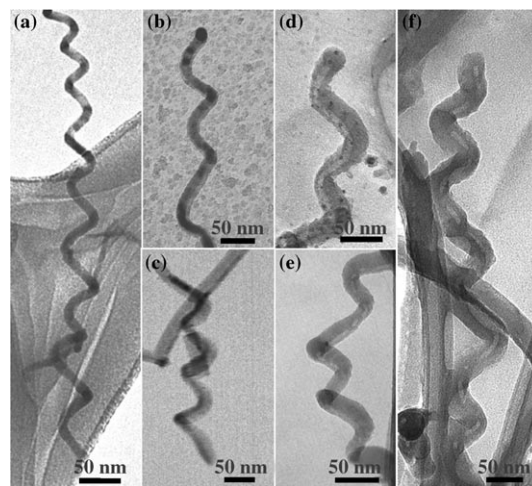


**Figure 7.** a) TEM image of a single ZnO nanohelix; b, c) TEM images of ZnO-SiC core-shell nanohelices; d-f) TEM images of SiC hollow nanohelices.

ZnO nanohelices with average diameters of  $\approx 10$  nm. Figure 7b and c shows two ZnO-SiC core-shell nanohelices after coating with SiC. After etching away the ZnO cores using HCl solution, SiC tubular nanohelices were produced (Figure 7d-f).

In summary, we have demonstrated a general technique for fabricating hollow nanostructures of desired shapes. One, two, and three-dimensional complex-shaped ZnO nanostructures have been replicated by SiC shells via PECVD at rather low temperatures. After dissolving the templates, shape-defined, rigid, robust, and high-quality SiC-shelled nanostructures were fabricated. This is one of the most effective techniques for producing hollow nanostructures. The SiC-shell nanostructures could have potential applications as space-confined nanoreactors, catalysts, nanofluidic channels, and in drug delivery.

## Experimental Section

**Synthesis of ZnO nanobelts:** Commercial ZnO ( $\approx 2.0$  g) was loaded as the source material into an alumina boat positioned at the center of the alumina tube furnace, where the temperature, pressure, and evaporation time were controlled. The tube furnace was heated to  $1375^\circ\text{C}$  at a rate of  $50^\circ\text{C min}^{-1}$  and held at the peak temperature for 2 h under a constant pressure of 75 Torr and an Ar flow rate of 50 sccm (standard cubic centimeters per minute). Finally, ZnO nanobelts were grown on the alumina substrates placed at the downstream end of the alumina tube, where the deposition temperature was around  $600^\circ\text{C}$ .

**Synthesis of tin-catalyzed ZnO nanowires:**<sup>[15b]</sup> A mixture of commercial ZnO, SnO<sub>2</sub>, and graphite powders in a ratio of Zn/

Sn/C 2:1:1 was placed as the source material in an alumina boat positioned at the center of the alumina tube furnace. The furnace was then heated to  $\approx 1150^\circ\text{C}$  for 60 min under a constant pressure of 200 mbar (1 mbar = 0.75 Torr) and an Ar flow rate of 20 sccm. The tin-catalyzed ZnO nanowires were deposited onto alumina substrates located in a temperature range of 550–600  $^\circ\text{C}$ .

**Synthesis of ZnO nanocombs:**<sup>[16a]</sup> Commercial ZnO powder was loaded as the source material into an alumina boat and placed at the center of the tube furnace. The furnace was then heated to 1400–1450  $^\circ\text{C}$  with an Ar carrier gas flow rate of 50 sccm and a pressure of 200–250 mbar. With constant pressure and gas flow rate, the evaporation process was maintained for 100–150 min. The ZnO nanocombs were then collected within a temperature range of 600–800  $^\circ\text{C}$ .

**Synthesis of ZnO nanojunctions:**<sup>[15c]</sup> Commercial ZnO and SnO<sub>2</sub> powders with a 1:1 weight ratio (5 g in total) were carefully mixed by grinding the powders for 15 min; the mixture was then loaded as the source material into an alumina boat and placed at the center of the tube. After evacuating the tube to  $2 \times 10^{-3}$  Torr, thermal evaporation was conducted at 1300  $^\circ\text{C}$  for 60 min under a pressure of 300–400 Torr and an Ar carrier gas flow rate of 50 sccm. The ZnO nanojunctions were grown within a temperature range of 700–800  $^\circ\text{C}$ .

**Synthesis of ZnO nanohelices:**<sup>[18]</sup> A mixture of source materials consisting of powdered ZnO (0.6 g), Li<sub>2</sub>CO<sub>3</sub> (0.3 g), and Ga<sub>2</sub>O<sub>3</sub> (0.1 g) was placed at the center of an alumina tube inserted into a horizontal tube furnace. The tube furnace was then heated to 1000  $^\circ\text{C}$  at a rate of 30  $^\circ\text{C min}^{-1}$  and held at the peak temperature for 2 h with the chamber pressure kept at 200 Torr and with an Ar flux of approximately 25 sccm. Finally, the ZnO nanohelices were grown on the silicon substrates placed at the downstream end of the alumina tube where the deposition temperature was 250–350  $^\circ\text{C}$ .

**Synthesis of ZnO–SiC core–shell nanostructures and SiC tubelike nanostructures:** The ZnO–SiC core–shell nanostructures were prepared via PECVD. The alumina substrates containing the ZnO nanostructures were placed in the PECVD chamber, pre-pumped to 10 mTorr. SiH<sub>4</sub> (5% in He) and CH<sub>4</sub> gases were then introduced as precursors into the chamber with flow rates of 300 and 100 sccm, respectively. The PECVD was then run at a power of 50 W for 10 min during which the precursors were converted into a plasma state under the radio frequency (RF) operating voltage. Silicon ions reacted with those of carbon to form SiC, which was deposited on the surface of the ZnO nanostructures at a temperature of 250–300  $^\circ\text{C}$ . Finally, ZnO–SiC core–shell nanostructures were formed and the color of the nanostructures on the alumina substrates turned from white to pale yellow.

**Synthesis of SiC tubelike nanostructures:** SiC nanotubes were obtained by removal of the ZnO core in a dilute HCl solution. In this process, the core–shell nanostructures were firstly dispersed in ethanol, and then diluted HCl solution (0.2 mol L<sup>-1</sup>) was added to the ethanol solution. The reaction was allowed to proceed at room temperature. After  $\sim 2$  min, the solution turned transparent.

**Structure characterization:** The morphologies of the ZnO nanostructures were characterized by SEM (Leo 1530). The ZnO–SiC core–shell nanostructures and SiC-shell nanostructures were

characterized by TEM (Hitachi 2000 and JEOL 100C). The chemical composition of the ZnO–SiC core–shell nanostructure was analyzed by the EDX equipment on the Hitachi TEM.

## Keywords:

core–shell materials • nanostructures • silicon carbide • templates • zinc oxide

- [1] a) F. Caruso, *Adv. Mater.* **2001**, *13*, 11; b) E. Donath, G. B. Sukhorukov, F. Caruso, S. A. Davis, H. Möhwald, *Angew. Chem.* **1998**, *110*, 2323; *Angew. Chem. Int. Ed.* **1998**, *37*, 2201.
- [2] C. C. Chen, Y. C. Liu, C. H. Wu, C. C. Yeh, M. T. Su, Y. C. Wu, *Adv. Mater.* **2005**, *17*, 404.
- [3] E. B. Kmieć, *Am. Sci.* **1999**, *87*, 240.
- [4] a) J. N. Wohlstädter, J. L. Wilbur, G. B. Sigal, H. A. Biebuyck, M. A. Billadeau, L. Dong, A. B. Fischer, S. R. Gudiband, S. H. Jameison, J. H. Kenten, J. Leginus, J. K. Leland, R. J. Massey, S. J. Wohlstädter, *Adv. Mater.* **2003**, *15*, 1184; b) A. Bianco, M. Prato, *Adv. Mater.* **2003**, *15*, 1765; c) V. Lovat, D. Pantarotto, L. Lagostena, B. Cacciari, M. Grandolfo, M. Righi, G. Spalluto, M. Prato, L. Ballerini, *Nano Lett.* **2005**, *5*, 1107.
- [5] a) R. Fan, R. Kamik, M. Yue, D. Y. Li, A. Majumdar, P. D. Yang, *Nano Lett.* **2005**, *5*, 1633; b) P. Kohli, C. C. Harrell, Z. H. Cao, R. Gasparac, W. H. Tan, C. R. Martin, *Science* **2004**, *305*, 984.
- [6] S. B. Lee, D. T. Mitchell, L. Trofin, T. K. Nevanen, H. Soderlund, C. R. Martin, *Science* **2002**, *296*, 3198.
- [7] X. Y. Kong, Z. L. Wang, J. Wu, *Adv. Mater.* **2003**, *15*, 1445.
- [8] J. Goldberger, R. R. He, Y. F. Zhang, S. Lee, H. Q. Yan, H. J. Choi, P. D. Yang, *Nature* **2003**, *422*, 599.
- [9] *Properties of Silicon Carbide* (Ed.: G. L. Harris), Institution of Engineering and Technology, London, **1995**.
- [10] a) E. Borowiak-Palen, M. H. Ruemmel, T. Gemming, M. Knupfer, K. Biedermann, A. Leonhardt, T. Pihler, R. J. Kalenczuk, *J. Appl. Phys.* **2005**, *97*, 056102; b) T. Taguchi, N. Igawa, H. Yamamoto, S. Shamoto, S. Jitsukawa, *Phys. E* **2005**, *28*, 431.
- [11] J. Q. Hu, Y. Bando, J. H. Zhan, D. Goberg, *Appl. Phys. Lett.* **2004**, *85*, 2923.
- [12] a) X. H. Sun, C. P. Li, W. K. Wong, N. B. Wong, C. S. Lee, S. T. Lee, B. K. Teo, *J. Am. Chem. Soc.* **2002**, *124*, 14464; b) N. Leller, C. P. Huu, G. Ehret, V. Keller, M. J. Ledoux, *Carbon* **2003**, *41*, 3131; c) C. Pham-Huu, N. Keller, G. Ehret, M. J. Ledoux, *J. Catal.* **2001**, *200*, 400.
- [13] a) X. Y. Kong, Z. L. Wang, *Nano Lett.* **2003**, *3*, 1625; b) X. Y. Kong, Y. Ding, R. S. Yang, Z. L. Wang, *Science* **2004**, *303*, 1348; c) P. X. Gao, Z. L. Wang, *Small* **2005**, *1*, 945.
- [14] P. X. Gao, Y. Ding, W. J. Mai, W. L. Hughes, C. S. Lao, Z. L. Wang, *Science* **2005**, *309*, 1700.
- [15] a) P. X. Gao, Y. Ding, Z. L. Wang, *Nano Lett.* **2003**, *3*, 1315; b) Y. Ding, P. X. Gao, Z. L. Wang, *J. Am. Chem. Soc.* **2004**, *126*, 2066; c) P. X. Gao, Z. L. Wang, *J. Phys. Chem. B* **2002**, *106*, 12653; d) P. X. Gao, Z. L. Wang, *Appl. Phys. Lett.* **2004**, *84*, 2883.
- [16] a) C. S. Lao, P. X. Gao, R. S. Yang, Y. Zhang, Y. Dai, Z. L. Wang, *Chem. Phys. Lett.* **2005**, *417*, 359; b) Z. L. Wang, X. Y. Kong, J. M. Zuo, *Phys. Rev. Lett.* **2003**, *91*, 185502.
- [17] X. D. Wang, C. J. Summers, Z. L. Wang, *Nano Lett.* **2004**, *4*, 423.
- [18] R. Yang, Y. Ding, Z. L. Wang, *Nano Lett.* **2004**, *4*, 1309.
- [19] X. Y. Kong, Y. Ding, R. S. Yang, Z. L. Wang, *Science* **2004**, *303*, 1348.
- [20] Z. W. Pan, Z. R. Dai, Z. L. Wang, *Science* **2001**, *291*, 1947.
- [21] Y. H. Gao, Y. Bando, *Nature*, **2002**, *415*, 599.

Received: February 28, 2006

Published online on August 7, 2006